

## Optimization and application of a gel polymer electrolyte in solid state super capacitors with graphite electrodes

Buddhika P. Gunasekara<sup>1a</sup>, Kumudu S. Perera<sup>\*2</sup>,  
Kamal P. Vidanapathirana<sup>2b</sup> and K. Vignarooban<sup>1c</sup>

<sup>1</sup> Department of Physics, University of Jaffna, Jaffna, Sri Lanka

<sup>2</sup> Department of Electronics, Wayamba University of Sri Lanka, Kuliyaipitiya, Sri Lanka

(Received February 1, 2020, Revised December 28, 2021, Accepted March 27, 2021)

**Abstract.** The prime objective of the present study is to exploit a user friendly, inexpensive all solid state super capacitor using a suitable electrolyte and electrodes. A gel polymer electrolyte (GPE) consisted with polyvinylidene fluoride-co-hexafluoropropylene (PVdF), ethylene carbonate (EC), propylene carbonate (PC) and zinc trifluoromethane sulfonate ( $Zn(CF_3SO_3)_2$ -ZnTF) was prepared using solvent casting method and its properties were optimized by varying the composition. The composition of 16 PVdF : 22 ZnTF : 31 EC : 31 PC (weight %) exhibits the optimum room temperature conductivity of  $3.09 \times 10^{-3} \text{ Scm}^{-1}$ . It is purely an ionic conductor having a negligible electronic conductivity. In addition, it was possible to obtain a thin, mechanically stable film. The electrodes were prepared using Sri Lankan natural graphite (NG) with a polymer binder. Eventhough there are reports about natural graphite based super capacitors, Sri Lankan natural graphite has not been considered for super capacitors at a large scale. The main reason for turning towards natural graphite is to reap the benefits of low cost as well as the safety. In order to optimize the electrode properties, the ratio between graphite and polymer binder (in weight basis) was changed. The polymer binder used was polytetrafluoroethylene (PTFE). Super capacitor fabricated with the electrode of the composition, NG : PTFE = 90:10 shows the maximum single electrode specific capacitance ( $2.58 \text{ Fg}^{-1}$ ). The fabricated device retains for continuous charge discharge operation with a minimum performance reduction.

**Keywords:** gel polymer electrolytes; natural graphite; super capacitors; binders; PTFE; specific capacitance

### 1. Introduction

At universal level, there exists a soaring demand for uninterrupted power due to emergence of diverse applications in modern luxurious life patterns. Since long ago, fossil fuel has been consumed to accommodate the demand for power and as a result, now they are predicted to be in an endangered state (Winter and Brodd 2004, Sheha 2013). This has motivated the researchers to seek alternative energy sources. And also due to the high rising concerns over the eco-friendly concepts, priority had to be given to energy sources which are inherently safe. In this regard, solar and wind energy has received a notable attention. However, their native intermittent nature with

---

\*Corresponding author, Professor, E-mail: [kumudu31966@gmail.com](mailto:kumudu31966@gmail.com)

<sup>a</sup> [prasadgunasekera2292@gmail.com](mailto:prasadgunasekera2292@gmail.com)

<sup>b</sup> [kamalpv41965@gmail.com](mailto:kamalpv41965@gmail.com)

<sup>c</sup> [kvignarooban@gmail.com](mailto:kvignarooban@gmail.com)

the dependence on location and time, has highlighted the necessity for storing energy in order to provide a continuous supply. For this purpose, batteries and capacitors have been used all over the world based on various materials.

Over the last several years, due to the significant breakthroughs in science and technology, cry for energy did rise up so high that contribution from batteries and capacitors is not capable to tolerate the thirst. As a result, super capacitors have been introduced as talented substitutes with remarkable features in terms of higher power density than batteries and higher energy density than conventional capacitors (Tey *et al.* 2016, Subramanian *et al.* 2007). With the economical constraints blended with safety issues, there is a growing demand at present for developing low cost and environmental friendly super capacitors. To meet those challenges, a great amount of scientific research has been focused towards exploiting novel materials (Aval 2018). Sri Lanka is blessed with so many natural resources. Among them, graphite is one of such natural resources found in different locations. Sri Lankan natural graphite (NG) has been used in a large number of fields other than energy and power sector. That is mainly because its potential to serve in that field has not been discovered until recently. However, commercial graphite has been used by several research groups for fabricating super capacitors. Many of those super capacitors are anyway based on liquid electrolytes which present insurmountable obstacles for the effective and efficient performance. Solid electrolytes are not competing for serving in many devices due to their low ionic conductivity. In the recent past, gel polymer electrolytes have received an intense interest as a class of materials lying in between solid and liquid electrolytes (Song *et al.* 2003, Tripathi *et al.* 2013).

In this study, attempts were launched to identify the viability of Sri Lankan NG to be used for all solid state super capacitors. For that, a gel polymer electrolyte (GPE) was employed in place of a liquid electrolyte. Compositions of NG based electrode as well as GPE were optimized to improve the performance of the super capacitor.

## **2. Experimental**

### *2.1 Preparation and optimization of the electrodes*

NG received from Bogala Graphite mines in Sri Lanka, polytetrafluoroethylene (PTFE) (Aldrich) and isopropanol (Aldrich) were used as received without any prior treatment. Required amounts of NG and PTFE were weighed and magnetically stirred first in isopropanol for 6 hours. Then the mixture was sonicated further. The resultant slurry was spread on fluorine doped tin oxide (FTO) glass plates using doctor blade method. They were allowed to dry in normal atmosphere. Electrodes were prepared having different NG : PTFE ratios. Using them, super capacitors were fabricated to find the composition that shows the optimum performance.

### *2.2 Preparation of the GPE*

GPE was prepared using polyvinylidene fluoride-co-hexafluoropropylene (PVdF-co-HFP) as the host polymer, ethylene carbonate (EC) and propylene carbonate (PC) as solvents, and zinc trifluoromethane sulfonate ( $\text{Zn}(\text{CF}_3\text{SO}_3)_2 - \text{ZnTf}$ ) as the salt. All the chemicals were from Aldrich and used as received. First, required amount of ZnTF was dissolved in EC and PC by magnetic stirring and at the same time, PVdF-co-HFP was also dissolved in acetone by magnetic stirring for about 3 hours. After the materials have been completely dissolved, both solutions were mixed

together and the final solution was further stirred for about 3 hours. The resulted homogeneous mixture was poured in to a petri dish and kept at room temperature for solvent evaporation slowly overnight. Thereby, it was possible to obtain a bubble free, thin but mechanically stable film.

### **2.3 Optimization and characterization of GPE**

A circular shape sample was cut from the electrolyte film and it was loaded in between two well cleaned stainless steel dice inside a spring loaded sample holder. Impedance data were gathered from room temperature by placing the sample holder in a glass tube furnace (Sibata) and using a frequency response analyser (Metrohm M101). Samples were prepared varying the salt concentration. For each sample, impedance data were gathered and analysed. The composition that showed the highest conductivity value at each temperature was used for further analysis. A GPE sample was sandwiched in between two stainless steel electrodes and a DC bias potential of 1 V was applied. Current variation through the setup was monitored with time. Electrochemical stability window of the GPE was determined using linear Sweep Voltammetry (LSV) technique. For that, a GPE sample was assembled in between a Zn electrode and a stainless steel (SS) electrode. SS electrode was used as the working electrode and the Zn electrode was used as the reference and counter electrodes. A computer controlled Metrohm Autolab M101potentiostat was used to obtain the current variation with voltage at the scan rate of 10 mVs<sup>-1</sup>.

### **2.4 Fabrication and characterization of super capacitors**

A GPE having an area of cross section 1 cm<sup>2</sup> was sandwiched in between two ideal NG electrodes. Electrochemical Impedance Spectroscopy (EIS) technique was used to select the electrode composition that shows the highest super capacitor performance. For each electrode composition, impedance data were collected using a Metrohm Frequency Response Analyser (M101) in the frequency window 400 KHz – 0.005 Hz at room temperature.

The super capacitor which showed the highest performance from EIS test, was further analysed using Cyclic Voltammetry technique and Galvanostatic Charge Discharge (GCD) technique. Cyclic voltammetry tests were carried out using a three-electrode setup where one electrode was used as the working electrode and the other was served as reference and counter electrode. Varying the scan rates, cyclic voltammogrammes (CVs) were obtained within the potential window, 0.1 V – 2.0 V using a computer controlled potentiostat (Metrohm 101). Continuous cycling was done in the same potential window at the scan rate selected from the previous study. Galvanostatic charge-discharge (GCD) test was performed to observe the charge-discharge characteristics under the constant current of 1×10<sup>-4</sup> A in the potential window 0.1 V – 2.0 V by using Metrohm-M101 potentiostat module.

## **3. Results and discussion**

### **3.1 Optimization of GPE**

From impedance data, Nyquist graphs were plotted with real and imaginary impedance values. Conductivities were calculated at each temperature using Nyquist plots and the equation

$$\sigma = (t/R_bA)$$

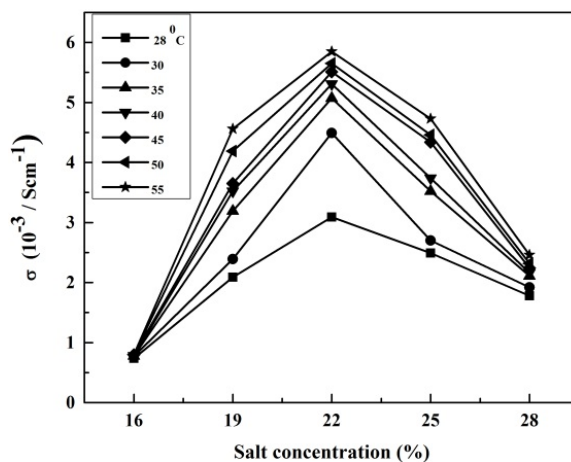


Fig. 1 Variation of conductivity with the salt concentration at different temperatures

where  $R_b$  is the bulk electrolyte resistance obtain from Nyquist plots,  $t$  and  $A$  are the thickness and cross section area of GPE respectively (Margaret and Suthanthiraraj 2013).

Fig. 1 shows the variation of conductivity with the salt concentration at each temperature.

At low salt concentrations, samples are having lower conductivities. As the salt concentration increases, conductivity also increases. It is a well-known fact that conductivity is governed mainly by two factors namely charge carrier concentration and mobility. With increasing salt concentration, population of charge carriers increases and as a result, conductivity increases. Further increment of salt concentration may result more charge carriers which promotes ion association forming ion clusters. They do not contribute for conduction being in neutral state. On the other hand, higher charge carrier concentrations may increase viscosity disturbing mobility of charge carriers. Due to those reasons, conductivity can decrease when salt concentration increases. It is clearly seen at each temperature, GPE having the salt concentration of 22% bears the maximum conductivity of  $3.09 \times 10^{-3} \text{ Scm}^{-1}$ . The corresponding composition of the GPE is 16 PVdF : 22 ZnTF : 31 EC : 31 PC (weight %).

### 3.2 Characterization of GPE

Fig. 2 illustrates the conductivity variation of GPE sample, 0.5 PVdF : 0.7 ZnTF : 1 EC : 1 PC with the temperature.

As temperature increases, the conductivity increases. It might be due to gain of thermal energy by charge carriers and becoming more energetic resulting higher mobility. This gives rise to a noticeable conductivity increment.

The non linear pattern of the variation suggests that conductivity mechanism of GPE follows Vogel Tammna Fulcher (VTF) behaviour which is commonly observed for viscous, amorphous systems [Pandey *et al.* 2011]. It can be proposed that ion conduction mechanism takes place via free volumes created by polymer matrix. As the temperature is increased, polymer can expand easily and produce free volume (Rajendran *et al.* 2001). Data were fitted with VTF equation to determine activation energy and pre-exponential factor. Calculated activation energy is 0.08 eV which is very small implying the easy ion migration in the electrolyte. Pre-exponential factor was found to be  $0.39 \text{ Scm}^{-1}\text{K}^{1/2}$ .

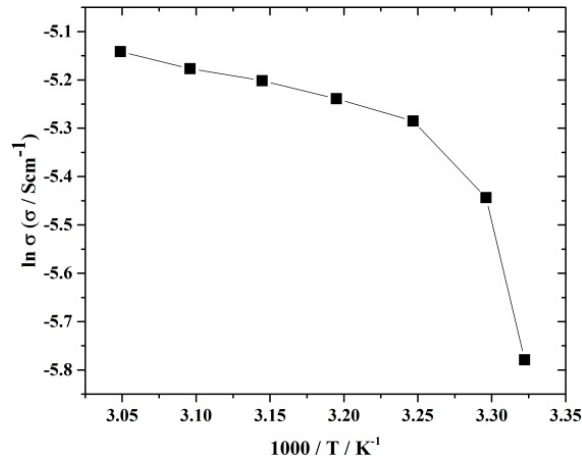


Fig. 2 Conductivity variation of GPE sample, 16 PVdF : 22 ZnTF : 31 EC : 31 PC (weight %) with the temperature

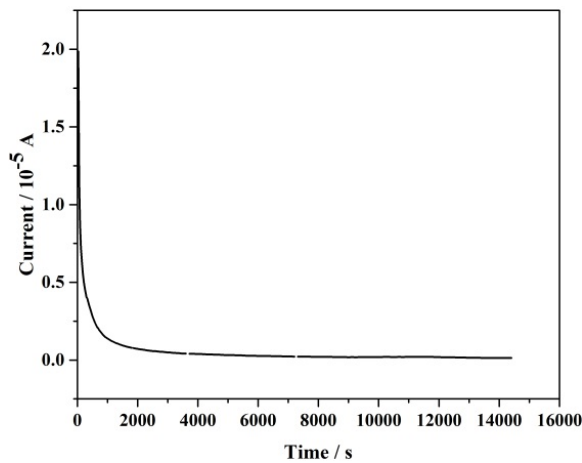


Fig. 3 DC polarization curve for the GPE sample, 16 PVdF : 22 ZnTF : 31 EC : 31 PC (weight %) under a 1 V of DC bias potential

Fig. 3 shows the DC polarization curve obtained for the GPE under a 1 V of DC bias potential.

As soon as the application of the bias potential, a sudden sharp drop of current is seen. It is thereafter followed by a stable current. The initial current decrease is due to the polarization of ions which are blocked by the stainless steel electrodes. A continuous current flow is present after the drop due to the movement of electrons.

The ionic transference number,  $t_i$  can be calculated as

$$t_i = (I_t - I_s) / I_t$$

where  $I_t$  and  $I_s$  are total current and stable current values respectively. The value of  $t_i$  is 0.99 which confirms the fact that GPE is purely an ionic conductor (Sharma and Hashmi 2018). This feature is very much essential to be used the GPE as an electrolyte.

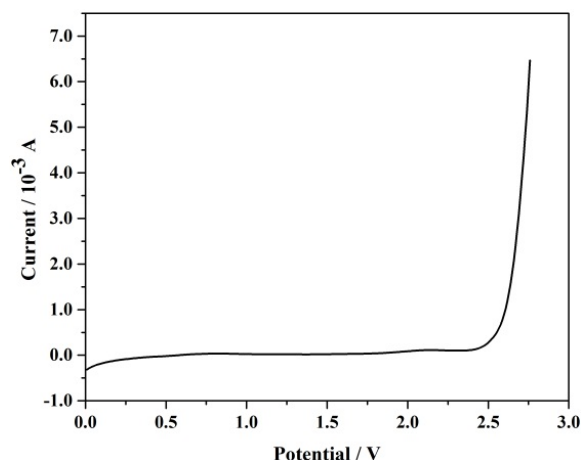


Fig. 4 Linear sweep voltammogramme for the GPE sample sample, 16 PVdF : 22 ZnTF : 31 EC : 31 PC (weight %)

The potential range in which no any reactions are assumed to be taken place is considered as the electrochemical stability window (ESW). With regard to applications, it is also preferred to have a wider ESW. Determination of ESW is done by linear sweep voltammetry. In the resulting voltammogramme, the region where the current remains constant is taken as the ESW. Fig. 4 shows the resulted linear sweep voltammogramme for the GPE investigated in the present study.

According to that, anodic onset of the current which is treated as the decomposition voltage of the GPE is found around 2.25 V. This value is taken as the maximum value for safe usage (Aravindan *et al.* 2009). ESW of the GPE under study was taken as from 0.1 to 2.25 V where the current varies constantly.

### 3.3 Characterization of EDLC

#### 3.3.1 Electrochemical impedance spectroscopy

Single electrode specific capacitance ( $C_{sc}$ ) can be derived from Nyquist plots (Fig. 5(a)) as

$$C_{sc} = 1/2\pi f z''$$

where  $Z''$  is the value of the imaginary part of the complex impedance,  $Z$  corresponding to the lowest frequency,  $f$  (Prabaharan *et al.* 2006). This equation was rearranged to plot a graph between  $Z''$  and  $1/2\pi f$  in low frequency region where the capacitive features become dominant and then to find  $C_{sc}$  using the gradient. The reason behind this is to generalize the calculation of  $C_{sc}$ . By plotting such graphs for each EDLC, the highest  $C_{sc}$  was determined. Fig. 5(b) illustrates the respective graph for the EDLC fabricated with the electrode having the composition, NG : PTFE = 90 : 10.

With the straight line, the gradient was calculated and using that,  $C_{sc}$  was found.

Fig. 6 shows the variation of  $C_{sc}$  with different NG weight percentages.

When increasing NG amount,  $C_{sc}$  initially increases but after the ratio of NG : PTFE = 90 : 10,  $C_{sc}$  reduces. The maximum  $C_{sc}$  is  $2.58 \text{ Fg}^{-1}$ . Upon increasing NG, the storage of charges may be facilitated. But, when the effect of binder reduces with more NG, the storage process may be

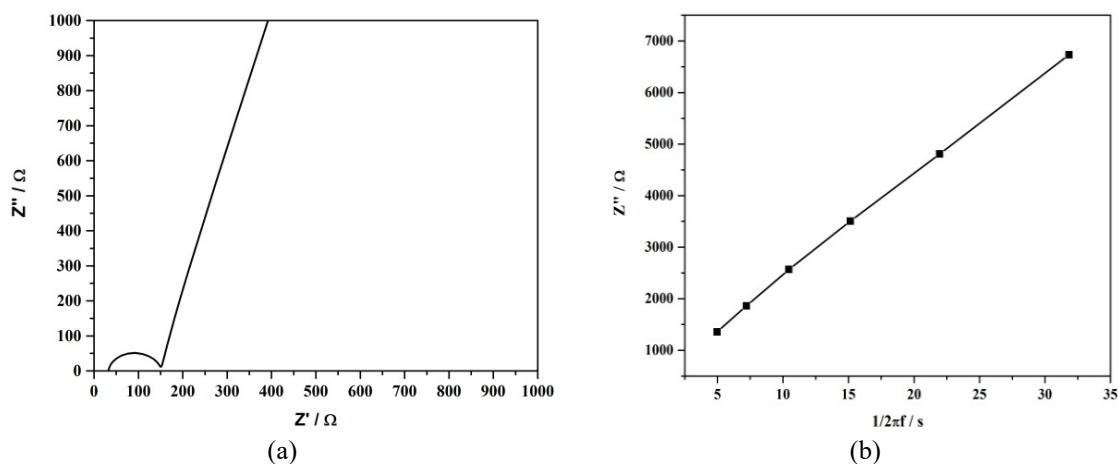


Fig. 5 (a) A resulted impedance plot; (b) the graph between  $Z''$  and  $1/2\pi f$  in low frequency region for the EDLC with the electrode composition, NG : PTFE = 90 : 10

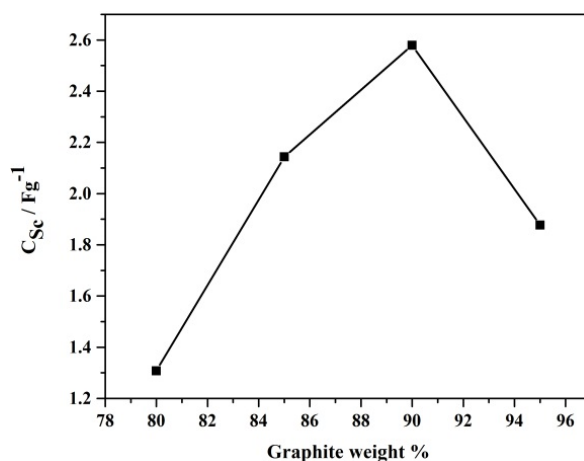


Fig. 6 The variation of  $C_{sc}$  with different NG weight percentages

disturbed. This is an evidence for the importance of a certain amount of a binder with NG. In general, binders are playing a great role for retaining the active material in the electrode during operation and at the same time, they should not cover the effective surface areas or pores giving rise to lower performance (Ranade *et al.* 2011).

Various binders such as polyvinylidene fluoride (PVdF) and PTFE have been investigated by several groups and Zhu *et al.* have reported that PTFE is more suitable than PVdF. In addition, they have also reported that 10% of PTFE with the active material is the optimum amount that should be present in the electrode (Zhu *et al.* 2016). This is very much agreeable with the observation obtained by the present study.

### 3.3.2 Cyclic voltammetry

Fig. 7 shows the cyclic voltammogramme (CV)s obtained at different scan rates.

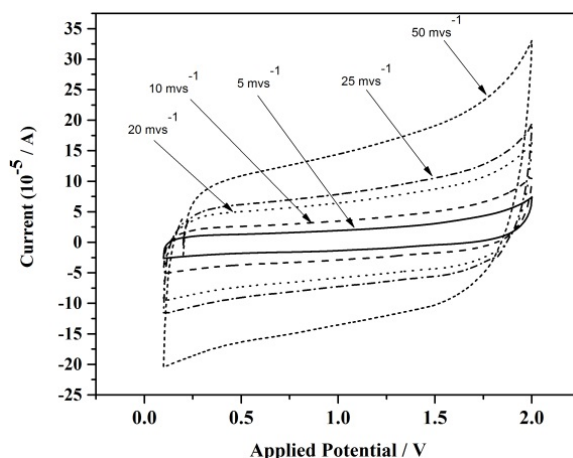


Fig. 7 Cyclic voltammogramme (CV)s obtained for the EDLC at different scan rates

All CVs are in rectangular shape which is a characteristic feature of a super capacitor having carbon based electrodes (Pal and Ghosh 2018). It is a well-known fact that peaks in a CV symbolize the redox reactions in a particular device (Tey *et al.* 2016). The charge storage mechanism in super capacitors with carbon based electrodes relies on accumulation of charges on the electrolyte electrode interface only. There is no redox reaction take place for charge storage. Hence, no peaks are appearing in that type of super capacitor (Das and Ghosh 2017). None of the resulted CV has cathodic and anodic peaks. This conforms that only charge accumulation takes place in the fabricated graphite super capacitors. At slow scan rates, CVs are of near symmetric around zero current axis. This is an evidence for the good reversibility of the charge storage process (Wang *et al.* 2012). When the scan rate is increased, a distortion of the rectangular shape occurs.

Fig. 8 depicts the variation of  $C_{sc}$  with scan rate.

The single electrode specific capacitance ( $C_{sc}$ ) was calculated using the equation

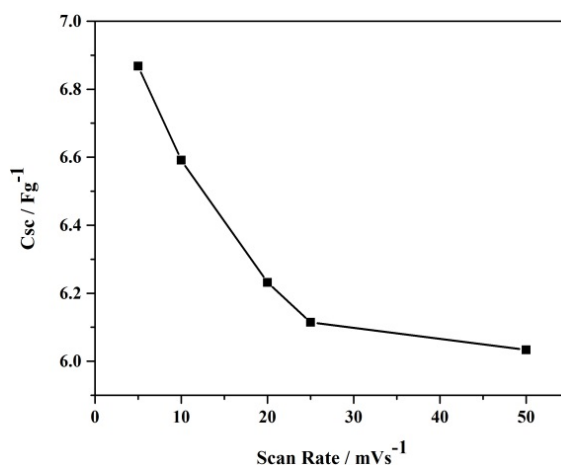


Fig. 8 Variation of  $C_{sc}$  of the EDLC with scan rate



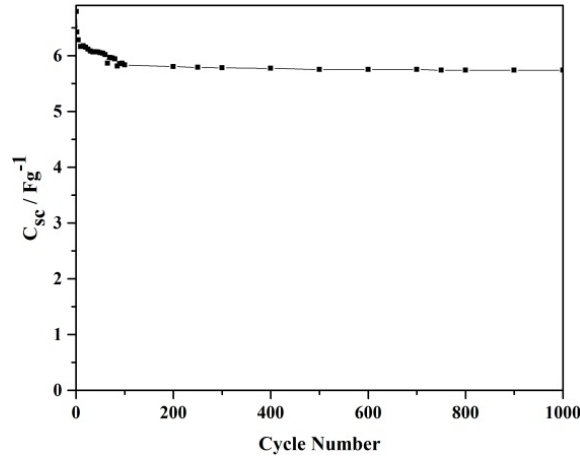


Fig. 9 Variation of C<sub>sc</sub> of the EDLC upon continuous cycling

$$C_{sc} = 2(\int IdV)/\Delta VSm$$

where  $\int IdV$  is the area of  $CV$ ,  $m$  is the single electrode mass,  $S$  is the scan rate and  $\Delta V$  is the width of the potential window.

Reduction of  $C_{sc}$  is seen confirming the fact that higher scan rates significantly lower the performance. At high scan rates, electrochemical kinetics cannot follow the fast potential change and as a result, ion movement becomes sluggish and also many of the micro pores in the active material are under-utilized (Kim *et al.* 2015). This reduces the performance very much.

Fig. 9 shows the variation of  $C_{sc}$  upon continuous cycling.

Upto about 100<sup>th</sup> cycle, there is a somewhat faster drop of  $C_{sc}$ . This may be possibly due to immature contacts at the initial stage. Upon continuous cycling, device gains maturity with the formation of proper contacts. After 100<sup>th</sup> cycle, the reduction is quite small. Jang *et al.* have predicted about detachment of active material from the substrate based on their observation of a steep capacitance reduction upon continuous cycling (Jang *et al.* 2013). Hence, the results of the present study can be used to prove the stability of the device.

### 3.3.3 Galvanostatic Charge Discharge (GCD) technique

Fig. 10(a) shows initial charge discharge curves and Fig. 10(b) illustrates the variation of single electrode discharge capacitance ( $C_d$ ) with continuous cycling.

Upto about 50<sup>th</sup> cycle, there is a capacitance fade at a considerable rate. But, after that, the reduction rate has become small. Soon after, the 150<sup>th</sup> cycle, there has been a sudden capacitance increase. This might arise due to a special characteristic of the electrolyte to recover from parasitic reactions. It is known as the self-healing property of an electrolyte. However, a slow capacitance reduction has taken place after that. This also elucidates the fact that the device has the capability to withstand for continuous operation. The material types are assumed to be highly responsible for cycling durability (Kim *et al.* 2015). Pseudo capacitive materials such as transition metal oxides and conducting polymers are having higher degradation rates (Chen *et al.* 2011). Accordingly, carbon based materials like NG are very much suitable for applications.

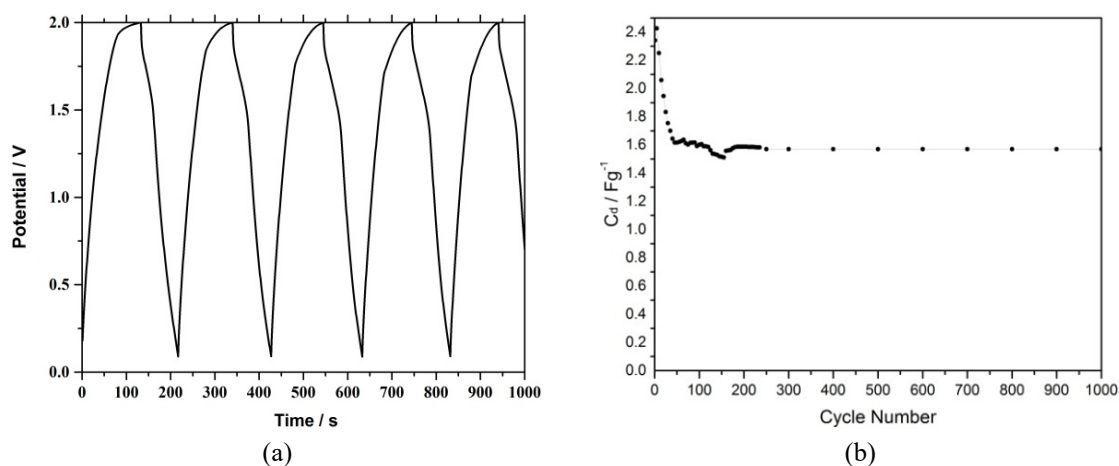


Fig. 10 (a) Initial charge discharge curves; (b) variation of single electrode discharge capacitance ( $C_d$ ) with continuous cycling

#### 4. Conclusions

The composition, 16 PVdF : 22 ZnTF : 31 EC : 31 PC (weight %) exhibits the optimum room temperature conductivity of  $3.09 \times 10^{-3} \text{ Scm}^{-1}$ . It is purely an ionic conductor having negligible electronic conductivity. ESW of the electrolyte is 0.1 V – 2.25 V. Super capacitor fabricated with the electrode of the composition, NG : PTFE = 90:10 shows the maximum single electrode specific capacitance ( $2.58 \text{ Fg}^{-1}$ ). When the super capacitor is cycled at higher scan rates, performance goes down. The fabricated device retains for continuous charge discharge operation with a minimum performance reduction. Further studies are carried out to improve the performance.

#### Acknowledgments

Financial assistance received from Wayamba University of Sri Lanka under the research grant, SRHDC/RP/04/17/01 is highly acknowledged.

#### References

- Aravindan, V., Karthikaselvi, G., Vickraman, P. and Naganandhini, S.P. (2009), “Polyvinylidene fluoride based novel polymer electrolytes for magnesium rechargeable batteries with  $\text{Mg}(\text{CF}_3\text{SO}_3)_2$ ”, *J. Appl. Polym. Sci.*, **112**, 3024-3029. <https://doi.org/10.1002/app.29877>
- Aval, L.F., Ghoranneviss, M. and Pour, G.B. (2018), “Graphite nano particle paper super capacitor based on gel electrolyte”, *Mater. Renew. Sustain. Energy*, **7**(4), 29-40. <https://doi.org/10.1007/s40243-018-0136-6>
- Chen, W., Rakhi, R.B., Hu, L., Xie, X., Cui, Y. and Alshareef, H.N. (2011), “High performance nano structured super capacitors on a sponge”, *Nano. Lett.*, **11**(12), 5165-5172. <https://doi.org/10.1021/nl2023433>
- Das, S. and Ghosh, A. (2017), “Solid polymer electrolyte based on PVdF-HFP and ionic liquid embedded with  $\text{TiO}_2$  nano particle for electric double layer capacitor application”, *J. Electrochem. Soc.*, **164**(13),

- F1348-F1353. <https://doi.org/10.1149/2.0561713jes>
- Jang, Y., Jo, J., Choi, Y.M., Kim, I., Lee, S.H., Kim, D. and Yoon, S.M. (2013), "Activated carbon nano composite electrodes for high performance super capacitors", *Electrochim. Acta.*, **102**, 240-245. <https://doi.org/10.1016/j.electacta.2013.04.020>
- Kim, B.K., Sy, S., Yu, A. and Zhang, J. (2015), *Handbook of Clean Energy Systems*, John Wiley and Sons Ltd.
- Pal, P. and Ghosh, A. (2018), "Highly efficient gel polymer electrolytes for all solid state electrochemical charge storage devices", *Electrochim. Acta*, **278**, 137-148. <https://doi.org/10.1016/j.electacta.2018.05.025>
- Pandey, K., Dwivedi, M.M., Asthana, N., Singh, M. and Agrawal, S.L. (2011), "Structural and ion transport studies in (100-x)PVdF+xNH<sub>4</sub>SCN gel electrolyte", *Mater. Sci. Appl.*, **2**(7), 721-728.
- Prabaharan, S.R.S., Vimala, R. and Zainal, Z. (2006), "Nanostructured meso porous carbon acelectrodes for super capacitors", *J. Power Sources*, **161**, 730-736. <https://doi.org/10.1016/j.jpowsour.2006.03.074>
- Priya, W.L.M. and Suthanthiraraj, S.A. (2013), "Preparation and characterization of polymer electrolytes containing poly(vinylidene fluoride-co-hexafluoropropylene) and zinc trifluoromethanesulfonate", *Che. Sci. Trans.*, **2**(4), 1232-1237.
- Rajendran, S., Mahendran, O. and Kannan, R. (2001), "Characterization of [(1-x)PMMA-xPVdF] polymer blend electrolyte with Li<sup>+</sup> ion", *Fuel*, **81**, 1077-1081. [https://doi.org/10.1016/S0016-2361\(01\)00178-8](https://doi.org/10.1016/S0016-2361(01)00178-8)
- Ranade, A.P., Jung, D.Y., Sammakia, B.G., Eilertsen, T. and Davis, T. (2011), "Optimization study of super capacitor electrode material composition and thickness for enhanced performance of the super capacitor", *Nano Science and Technology Institute*, **1**, 730-733.
- Sharma, J. and Hashmi, S. (2018), "Magnesium ion conducting gel polymer electrolyte nanocomposites : effect of active and passive nanofillers", *Polym. Composites.*, **40**(4), 1295-1306. <https://doi.org/10.1002/pc.24853>
- Sheha, E. (2013), "Prototype system for Mg/TiO<sub>2</sub> anatase batteries", *Int. J. Electrochem. Sci.*, **8**, 3653-3663.
- Song, M.K., Kim, Y.T., Kim, Y.T., Cho, B.W., Popov, B.N. and Rhee, H.W. (2003), "Thermally stable gel polymer electrolytes", *J. Electrochem. Soc.*, **150**(4), A439-A444. <https://doi.org/10.1149/1.1556592>
- Subramanian, V., Luo, C., Stephan, A.M., Nahm, K.S., Thomas, S. and Wei, B. (2007), "Super capacitors from activated carbon derived from banana fibers", *J. Phys. Chem.*, **111**, 7527-7531. <https://doi.org/10.1021/jp067009t>
- Tey, J.P., Careem, M.A., Yarmo, M.A. and Arof, A.K. (2016), "Durian shell based activated carbon electrode for EDLCs", *Ionics*, **22**/7, 1209-1217. <https://doi.org/10.1007/s11581-016-1640-2>
- Tripathi, S.K., Gupta, A., Jain, A. and Kumari, M. (2013), "Electrochemical studies on nanocomposite polymer electrolytes", *Indian J. Pure Appl. Phys.*, **51**, 358-361.
- Wang, Y., Cao, J., Zhou, Y., Ouyang, J.H., Jia, D. and Guo, L. (2012), "Ball milled graphite as an electrode material for high voltage super capacitor in neutral aqueous electrolyte", *J. Electrochem. Soc.*, **159**(5), A579-A583. <https://doi.org/10.1149/2.071205jes>
- Winter, M. and Brodd, R.J. (2004), "What are batteries, fuel cells and super capacitors", *Chem. Rev.*, **104**, 4245-4269. <https://doi.org/10.1021/cr020730k>
- Zhu, Z., Tang, S., Yuan, J., Qin, X., Deng, Y., Qu, R. and Haarberg, G.M. (2016), "Effects of various binders on supercapacitor performances", *Int. J. Electrochem. Sci.*, **11**, 8270-8279. <https://doi.org/10.20964/2016.10.04>